ELSEVIER

Applied Acoustics 57 (1999) 293–325

applied acoustics

# Numerical experiments for acoustic modes of a square cavity using the dual boundary element method

J.T. Chen[a,*], K.H. Chen[a], S.W. Chyuan[b]

[a]*Department of Harbor and River Engineering, National Taiwan Ocean University, Keelung 202, Taiwan*
[b]*Chunshan Institute of Science and Technology, Lungtan, Taiwan*

Received 10 November 1997; received in revised form 3 April 1998; accepted 23 September 1998

**Abstract**

The dual integral formulation for the Helmholtz equation for use in solving the acoustic modes of a two-dimensional square cavity is derived, and a general dual boundary element method (BEM) program is developed. Numerical experiments for the degenerate acoustic modes of a square cavity are performed. It is found that the degenerate modes can be distinguished by specifying the normalized boundary data at different boundary points using either the singular integral equation (UT method) or the hypersingular integral equation (LM method). This technique can be employed to determine the multiplicity of the eigenvalue. Two examples with Dirichlet and Neumann boundary conditions are given to show the validity of the proposed technique. Sensitivity and failure in determining the acoustic modes by specifying the normalized data at the boundary locations near and on the node are examined, respectively. Also, numerical results are obtained using finite element method (FEM) and analytical solutions for comparison. Good agreement between them is obtained. 

## 1. Introduction

The two numerical methods widely used in the analysis of interior acoustic fields are the finite element method (FEM) and boundary element method (BEM) [1]. Most BEM applications were based on the singular integral equation (UT method) instead of the hypersingular integral equation (LM method) of dual BEM.

* Corresponding author.

0003-682X/98/$–see front matter 
PII: S0003-682X(98)00062-0

The hypersingular integral was formulated by Hadamard [2] to treat the cylindrical wave equation by spherical means of descent. Also, Mangler derived the hypersingular kernel in solving the thin airfoil problem [3]. The improper integral was then defined by Tuck [4] as the "Hadamard principal value (H.P.V.)". In aerodynamics, it was termed "Mangler's principal value (M.P.V.)" [3,5]. Such a nonintegrable integral naturally arises in the dual integral formulation especially for problems with a degenerate boundary, e.g., crack problems in elasticity [6–11], heat flow through a baffle [12], Darcy flow around a cutoff wall [13,14], the aerodynamic problem of a thin airfoil [5] and acoustic waves impinging on a screen [15–18]. From the viewpoint of computational mechanics, the dual formulation also plays an important role in some other problems, e.g., the corner problem [19], adaptive BEM [20], and the exterior problem [21]. A general application of the hypersingular integral equation in mechanics was discussed in [22], and a review lecture on recent developments of dual BEM was presented by Chen [23]. When we combine the conventional integral equation, e.g., the Green's Identity or Somigliana Identity, with the hypersingular integral equation, we call the two equations "dual integral equations" due to the presence of a pair of continuous and discontinuous properties of the potential as the field point moves across the boundary [24–26]. From the above point of view, the definition of the dual integral equations is quite different from the conventional one used in crack elastodynamics by Buecker [27]. However, the dual equations in the present paper are independent with respect to each other for the undetermined coefficients of the complementary solution. The dual integral equations defined by Buecker resulted from the same equation but through collocation of different points. The present formulation has in total four kernel functions, which make possible a unified theory encompassing different schemes and interpretations. For elasticity, a detailed derivation can be found in [6]. In the dual formulation, the singularity order of hypersingularity for the kernel in the normal derivative of the double layer potential is stronger than that of the Cauchy type kernel by one. The paradox of the nonintegrable kernel is introduced due to the change of the integral and trace operators which is illegal from the point of view of the dual integral formulation [24]. In order to ensure a finite value, Leibnitz's rule should be considered as the derivative of the C.P.V. so that the boundary term $2/\epsilon$ can be included to compensate for the minus infinity. After the principal values are determined [28,29], the dual BEM can be easily implemented to solve the acoustic modes for a cavity.

For structural dynamics and acoustic problems, degenerate eigenfunctions occur in discrete systems and continuous systems for some limiting cases [30]. For example, a two-dimensional cavity with equal length and width results in a degenerate eigenvalue [31]. From the mathematical point of view, the degenerate eigenmodes result from an n by n matrix with a rank, $r$, which is smaller than $n-1$; i.e. this matrix has a nullity, $n-r$, which is larger than one. The multiplicity of the eigenvalue is equal to the number of nullity. The set of null solutions is used to construct the degenerate modes. From the theoretical point of view, Gladwell et al. [34] discussed the question of whether the level lines (contours) do or do not intersect each other

for the degenerate modes, i.e. whether the pressure field does or does not have saddle points. That paper concentrated on the qualitative properties of modes, but in so doing it resulted in a need for numerical studies on calculating mode shapes using, for instance, FEM or BEM. A discussion of the degenerate eigenvalues was also given by Laura et al. [35]. In the numerical approach using BEM[32], a technique in which the width was perturbated was used to separate the degenerate eigenvalues. As mentioned by Kamiya et al. [32], the direct determinant search method seems to be inadequate for the degenerate case; therefore, they transformed the nonlinear eigenvalue problem into a generalized eigenvalue problem to overcome this difficulty [33]. In the finite element method, different schemes for the degenerate modes were employed. Lin et al. [36] proposed a dummy link technique to determine the degenerate eigenmodes. Also, the finite element program [37] can deal with the problem of degenerate modes. This problem will be dealt with using a special technique in this study.

In this paper, we apply the dual integral formulation to solve the degenerate eigenfunctions of the two-dimensional Helmholtz equation for a square cavity. A general dual BEM program was developed. The role of the dual formulation for degenerate modes will be examined. The transcendental eigenequation will be constructed, and the degenerate eigenvalues will be still solved using the direct determinant search method. Since the multiplicity of the degenerate eigenvalue is greater than one, a special technique by setting a normalized value at different boundary locations will be employed to find the degenerate eigenfunctions. Also, the degenerate modes will be distinguished by using singular integral equation (UT method) and hypersingular integral equation (LM method). Illustrative problems for the degenerate modes of a square cavity will be given to check the validity of the proposed technique. Results obtained using dual BEM will be compared with those of analytical solutions and FEM results [37].

## 2. Dual integral formulation for the degenerate eigenfunctions of a square cavity

Consider an acoustic problem which has the following governing equation:

$$\nabla^2\phi(x)+k^2\phi(x)=0,\ x \text{ in } D, \tag{1}$$

where $D$ is the domain of interest, $x$ is the domain point, $\phi$ is the acoustic pressure and $k$ is the value of frequency divided by the speed of sound. The homogeneous boundary conditions can be shown as follows:

$$\phi(x)=0,\ x \text{ on } B_1, \tag{2}$$

$$\frac{\partial\phi(x)}{\partial n_x}=0,\ x \text{ on } B_2, \tag{3}$$

where $B_1$ is the essential boundary in which the acoustic pressure is prescribed, $B_2$ is the natural boundary where the normal derivative of the acoustic pressure in the $n_x$ direction is specified, and $B_1$ and $B_2$ construct the whole boundaries of the domain $D$.

The first equation of the dual boundary integral equations for the domain point can be derived from Green's third identity:

$$2\pi\phi(x) = \int_B T(s,x)\phi(s)\,\mathrm{d}B(s) - \int_B U(s,x)\frac{\partial\phi(s)}{\partial n_s}\,\mathrm{d}B(s), \quad x \in D, \tag{4}$$

where $x$ and $s$ denote the field point and the source point, respectively, and $T(s,x)$ is defined by

$$T(s,x) \equiv \frac{\partial U(s,x)}{\partial n_s}, \tag{5}$$

in which $n_s$ is the normal vector at the boundary point $s$, and $U(s,x)$ is the fundamental solution which satisfies

$$\nabla^2 U(x,s) + k^2 U(x,s) = \delta(x-s), \quad x \in D. \tag{6}$$

In Eq. (6), $\delta(x-s)$ is the Dirac-delta function. Since only Eq. (4) can not determine all the degenerate modes, another integral equation is necessary to be found. After taking the normal derivative with respect to Eq. (4), the second equation of the dual boundary integral equations for the domain point can be derived:

$$2\pi\frac{\partial\phi(x)}{\partial n_x} = \int_B M(s,x)\phi(s)\,\mathrm{d}B(s) - \int_B L(s,x)\frac{\partial\phi(s)}{\partial n_s}\,\mathrm{d}B(s), \quad x \in D, \tag{7}$$

where

$$L(s,x) \equiv \frac{\partial U(s,x)}{\partial n_x}, \tag{8}$$

$$M(s,x) \equiv \frac{\partial^2 U(s,x)}{\partial n_x \partial n_s}. \tag{9}$$

The explicit forms for the four kernel functions are summarized below:

$$U(s,x) = \frac{-i\pi H_0^{(1)}(kr)}{2}, \tag{10}$$

$$T(s,x) = \frac{-ik\pi}{2} H_1^{(1)}(kr)\frac{y_i n_i}{r}, \tag{11}$$

$$L(s,x)=\frac{ik\pi}{2}H_1^{(1)}(kr)\frac{y_i\bar{n}_i}{r}, \tag{12}$$

$$M(s,x)=\frac{-ik\pi}{2}\left\{-k\frac{H_2^{(1)}(kr)}{r^2}y_iy_jn_i\bar{n}_j+\frac{H_1^{(1)}(kr)}{r}n_i\bar{n}_i\right\}, \tag{13}$$

where $H_n^{(1)}(kr)$ is the $n$th order Hankel function of the first kind, $r$ is the distance between $x$ and $s$ points, $y_i=s_i-x_i$, $n_i,\bar{n}_i$ are the $i$th components of the normal vectors at $s$ and $x$, respectively.

By moving the field point $x$ in Eqs. (4) and (7) to the boundary, the dual boundary integral equations for the boundary point can be obtained as follows:

$$\pi\phi(x)=\text{C.P.V.}\int_B T(s,x)\phi(s)\,dB(s)-\text{R.P.V.}\int_B U(s,x)\frac{\partial\phi(s)}{\partial n_s}\,dB(s),\quad x\in B, \tag{14}$$

$$\pi\frac{\partial\phi(x)}{\partial n_x}=\text{H.P.V.}\int_B M(s,x)\phi(s)\,dB(s)-\text{C.P.V.}\int_B L(s,x)\frac{\partial\phi(s)}{\partial n_s}\,dB(s),\quad x\in B, \tag{15}$$

where R.P.V. is the Riemann principal value, C.P.V. is the Cauchy principal value and H.P.V. is the Hadamard (Mangler) principal value.

It must be noted that Eq. (15) can be derived by simply applying a normal derivative operator with respect to Eq. (14). Differentiation of the Cauchy principal value must be carried out carefully using Leibnitz's rule. The commutative property provides us with two alternatives for calculating the Hadamard principal value. The details can be found in [24]. Eqs. (4) and (7) are termed dual boundary integral equations for domain point, and Eqs. (14) and (15) are named dual boundary integral equations for the boundary point.

## 3. Dual boundary element formulation using constant element

After deriving the above compatible relationships of boundary data in Eqs. (14) and (15), the dual boundary integral equations can be discretized by using constant elements and the resulting algebraic system can be obtained as

$$[\bar{T}_{ij}]\{\phi\}=[U_{ij}]\left\{\frac{\partial\phi}{\partial n}\right\}, \tag{16}$$

$$[M_{ij}]\{\phi\}=[\bar{L}_{ij}]\left\{\frac{\partial\phi}{\partial n}\right\}, \tag{17}$$

where [ ] denotes a square matrix, a column vector and the elements of the square matrices are respectively,

$$U_{ij} = \text{R.P.V.} \int_{B_j} U(s_j, x_i)\, \mathrm{d}B(s_j), \tag{18}$$

$$\bar{T}_{ij} = -\pi\delta_{ij} + \text{C.P.V.} \int_{B_j} T(s_j, x_i)\, \mathrm{d}B(s_j), \tag{19}$$

$$\bar{L}_{ij} = \pi\delta_{ij} + \text{C.P.V.} \int_{B_j} L(s_j, x_i)\, \mathrm{d}B(s_j), \tag{20}$$

$$M_{ij} = \text{H.P.V.} \int_{B_j} M(s_j, x_i)\, \mathrm{d}B(s_j), \tag{21}$$

where $B_j$ denotes the $j$th element. All the above formulae can be separated into two parts, one is regular, the other is irregular. For the irregular part, the partial integration is employed to transform the hypersingular, strongly singular and weakly singular integrals into regular integrations. Therefore, the quadrature rule is used to determine all the integrals.

For the diagonal terms, $U_{ii}$, $T_{ii}$, $L_{ii}$ and $M_{ii}$, we have

(1) $U(s, x)$ kernel:

$$\begin{aligned} U_{ii} &= \frac{-i\pi}{2} \lim_{\epsilon \to 0} \int_{-0.5l}^{0.5l} H_0^{(1)}(k\sqrt{s^2+\epsilon^2})\, \mathrm{d}s \\ &= \frac{-i\pi}{2} \lim_{\epsilon \to 0} \left\{ \int_{-0.5l}^{-\sqrt{\epsilon}} H_0^{(1)}(k|s|)\, \mathrm{d}s \right. \\ &\quad \left. + \int_{-\sqrt{\epsilon}}^{\sqrt{\epsilon}} i\frac{2}{\pi} \ln\left(\frac{k}{2}\sqrt{s^2+\epsilon^2}\right) \mathrm{d}s + \int_{\sqrt{\epsilon}}^{0.5l} H_0^{(1)}(ks)\, \mathrm{d}s \right\} \\ &= \frac{-i\pi}{2} \lim_{\epsilon \to 0} \left\{ \int_{-0.5l}^{-\sqrt{\epsilon}} H_0^{(1)}(k|s|)\, \mathrm{d}s + 0 + \int_{\sqrt{\epsilon}}^{0.5l} H_0^{(1)}(ks)\, \mathrm{d}s \right\} \\ &= \frac{-i\pi}{2} \left\{ H_0^{(1)}\left(\frac{kl}{2}\right) l + k \int_{-0.5l}^{0.5l} H_1^{(1)}(k|s|)|s|\, \mathrm{d}s \right\} \end{aligned} \tag{22}$$

(2) $T(s, x)$ kernel:

$$\begin{aligned} T_{ii} &= \frac{i\pi k}{2} \lim_{\epsilon \to 0} \int_{-0.5l}^{0.5l} H_1^{(1)}(k\sqrt{s^2+\epsilon^2}) \frac{\epsilon}{\sqrt{s^2+\epsilon^2}}\, \mathrm{d}s \\ &= \frac{i\pi k}{2} \lim_{\epsilon \to 0} \int_{-\sqrt[4]{\epsilon}}^{\sqrt[4]{\epsilon}} \frac{i(-2)}{\pi k\sqrt{s^2+\epsilon^2}} \frac{\epsilon}{\sqrt{s^2+\epsilon^2}}\, \mathrm{d}s \\ &= \lim_{\epsilon \to 0} \arctan\frac{s}{\epsilon} \Big|_{-\sqrt[4]{\epsilon}}^{\sqrt[4]{\epsilon}} \\ &= \pi. \end{aligned} \tag{23}$$

(3) $L(s,x)$ kernel:

$$\begin{aligned} L_{ii} &= \frac{i\pi k}{2}\lim_{\epsilon\to 0}\int_{-0.5l}^{0.5l} H_1^{(1)}(k\sqrt{s^2+\epsilon^2})\frac{-\epsilon}{\sqrt{s^2+\epsilon^2}}\,ds \\ &= \lim_{\epsilon\to 0}\frac{-i\pi k}{2}\int_{-\sqrt[4]{\epsilon}}^{\sqrt[4]{\epsilon}}\frac{i(-2)}{\pi k\sqrt{s^2+\epsilon^2}}\frac{\epsilon}{\sqrt{s^2+\epsilon^2}}\,ds \\ &= -\pi. \end{aligned} \tag{24}$$

(4) $M(s,x)$ kernel:

$$\begin{aligned} M_{ii} &= \frac{-i\pi k}{2}\lim_{\epsilon\to 0}\int_{-0.5l}^{0.5l} -k\frac{H_2^{(1)}(k\sqrt{s^2+\epsilon^2})}{s^2+\epsilon^2}(-\epsilon)(-\epsilon) \\ &+ \frac{H_1^{(1)}(k\sqrt{s^2+\epsilon^2})}{\sqrt{s^2+\epsilon^2}}\,ds \\ &= \frac{-i\pi k}{2}\left\{-2H_1^{(1)}\left(\frac{kl}{2}\right)\right. \\ &\left. + k\left[H_0^{(1)}\left(\frac{kl}{2}\right) + k\int_{-0.5l}^{0.5l} H_1^{(1)}(k|s|)|s|\,ds\right]\right\}. \end{aligned} \tag{25}$$

## 4. Eigenequation for the eigenvalue problem obtained using dual BEM

For simplicity, problems with Dirichlet and the Neumann boundary conditions will be considered in this section. Numerical results obtained under either Dirichlet or Neumann conditions will be elaborated on later. After obtaining Eqs. (16) and (17) using dual BEM, we can obtain the transcendental equations as follows:

$$UT\,method: [\bar{T}_{ij}(k)]\phi_j = 0 \text{ for the Neumann problems}, \tag{26}$$

$$LM\,method: [M_{ij}(k)]\phi_j = 0 \text{ for the Neumann problems}, \tag{27}$$

$$UT\,method: [U_{ij}(k)]\left\{\left(\frac{\partial\phi}{\partial n}\right)_j\right\} = 0 \text{ for the Dirichlet problems}, \tag{28}$$

$$LM\,method: [\bar{L}_{ij}(k)]\left\{\left(\frac{\partial\phi}{\partial n}\right)_j\right\} = 0 \text{ for the Dirichlet problems}, \tag{29}$$

where $\phi_j$ is the boundary mode of the acoustic pressure, $(\partial\phi/\partial n)_j$ is the boundary mode of the normal flux of the acoustic pressure, and the eigenvalue, $k$, is imbedded in the elements of the matrix. The nontrivial eigensolution for $\phi_j$ and $(\partial\phi/\partial n)_j$ in Eqs. (26)–(29) only exists when the determinants of their influence matrix are zero.

Since either one of the two equations, UT or LM, can be selected, two alternative approaches, the UT and LM methods, are proposed. To solve for the eigenequation, a direct determinant search method is employed. After determining the eigenvalues, the boundary mode can be obtained by setting a normalized value to be one in any one element of the column vector of $\phi_j$. By changing the normalized data in one element of the vector $\phi_j$, different modes can be obtained if the eigenvalue is degenerate. By substituting the eigenvalue, boundary mode and known boundary condition into Eq. (4), the mode of the field can be obtained. It must be noted that sensitivity and failure in determining the boundary mode will occur if the locations of the normalized data are near and on the node, respectively. This phenomenon will be demonstrated in the following numerical experiments.

## 5. Acoustic analysis carried out using finite element method

Acoustics, "the science of sound", is the study of problems involving small vibrations in an inviscid fluid. Most of acoustic problems are generally modeled using the boundary element method; however, this method has not yet been implemented in the commercial code, ABAQUS. Thus, acoustic modeling in ABAQUS is restricted to the finite element approach. Acoustic pressure is the basic variable in acoustic analysis. For the Neumann boundary condition case, the gradient of the pressure normal to the plane, $\partial p/\partial n$, is zero. Since $\partial p/\partial n$ corresponds to surface "loading" in the acoustic problem, this boundary condition requires no data - it is an unloaded surface. This means that an arbitrary acoustic pressure value is present in the solution – the equivalent of a rigid body mode in a structural problem-resulting in a zero frequency mode. During the *FREQUENCY procedure, therefore, we introduce a shift of −10 cycles/s$^2$. This eliminates the difficulty of having a singularity in the matrix that must be solved during eigenvalue extraction. The negative shift ensures that the frequencies are still extracted in ascending order, starting with the zero frequency. For the problem with the Dirichlet boundary condition, $\phi=0$, on the surface, the *BOUNDARY option is employed. From the mathematical point of view,

Table 1
Eigenproblems using FEM, complex BEM and Real MRM

| | FEM | Complex BEM | Real MRM |
|---|---|---|---|
| State | $\underset{\sim}{X}$ | $\underset{\sim}{u},\underset{\sim}{t}$ | $\underset{\sim}{U},\underset{\sim}{t}$ |
| Eigenproblem | $\underset{\sim}{K}\underset{\sim}{X}=\omega^2\underset{\sim}{M}\underset{\sim}{X}$ | $\underset{\sim}{U}_c(\omega)\underset{\sim}{t}=\underset{\sim}{T}_c(\omega)\underset{\sim}{u}$ | $\underset{\sim}{U}_R(\omega)\underset{\sim}{t}=\underset{\sim}{T}_R(\omega)\underset{\sim}{u}$ |
| | | $\underset{\sim}{L}_c(\omega)\underset{\sim}{t}=\underset{\sim}{M}_c(\omega)\underset{\sim}{u}$ | $\underset{\sim}{L}_R(\omega)\underset{\sim}{t}=\underset{\sim}{M}_R(\omega)\underset{\sim}{t}=\underset{\sim}{M}_R(\omega)\underset{\sim}{u}$ |
| Eigenvalue | $\lambda=\omega^2$ | $\lambda=\omega^2$ | $\lambda=\omega^2$ |
| Eigenmode | $\underset{\sim}{X}$ | $\begin{Bmatrix}\underset{\sim}{u}\\ \underset{\sim}{t}\end{Bmatrix}$ | $\begin{Bmatrix}\underset{\sim}{u}\\ \underset{\sim}{t}\end{Bmatrix}$ |
| Eigenequation | $\underset{\sim}{A}\underset{\sim}{X}=\lambda\underset{\sim}{X}$ | $\underset{\sim}{A}(\lambda)\underset{\sim}{X}=\underset{\sim}{Q}$ | $(\underset{\sim}{A}_o+\lambda\underset{\sim}{A}_1+\lambda^2\underset{\sim}{A}_2+\cdots\lambda^n\underset{\sim}{A}_n)\underset{\sim}{X}=\underset{\sim}{Q}$ |

Table 2
Comparisons of the results by using exact solutions, UT method, LM method and ABAQUS

| Dirichlet problem ($\phi=0$ on $B$) | | | | | Neumann problem ($\frac{\partial\phi}{\partial n}=0$ on $B$) | | | | |
|---|---|---|---|---|---|---|---|---|---|
| *Eigenvalue* | $k_{mn}=\pi\sqrt{\left(\frac{m}{l}\right)^2+\left(\frac{n}{l}\right)^2}$ | | | | *Eigenvalue* | $k_{mn}=\pi\sqrt{\left(\frac{m}{l}\right)^2+\left(\frac{n}{l}\right)^2}$ | | | |
| *Eigenfunction* | $\rho_{mn}(x_1,x_2)=\sin\left(\frac{m\pi x_1}{l}\right)\sin\left(\frac{n\pi x_2}{l}\right)$ | | | | *Eigenfunction* | $\beta_{mn}(x_1,x_2)=\cos\left(\frac{m\pi x_1}{l}\right)\cos\left(\frac{n\pi x_2}{l}\right)$ | | | |
| | Exact sol. | UT | LM | ABAQUS | | Exact sol. | UT | LM | ABAQUS |
| $\lambda_1$ (1,1) | 240.4 | 240.3 | 240.3 | 243.2 | $\lambda_1^*$ (1,0),(0,1) | 170 | 169.9 | 169.9 | 172.0 |
| $\lambda_2^*$ (1,2),(2,1) | 380.1 | 380.4 | 380.9 | 384.6 | $\lambda_2$ (1,1) | 240.4 | 240.3 | 240.3 | 243.2 |
| $\lambda_3$ (2,2) | 480.8 | 481.1 | 480.5 | 486.5 | $\lambda_3^*$ (2,0),(0,2) | 340 | 341.8 | 341.8 | 344.0 |
| $\lambda_4^*$ (3,1),(1,3) | 537.6 | 537.9 | 537.3 | 544.1 | $\lambda_4^*$ (1,2),(2,1) | 380 | 379.9 | 379.9 | 384.6 |
| $\lambda_5^*$ (3,2),(2,3) | 612.9 | 613.1 | 612.2 | 620.3 | $\lambda_5$ (2,2) | 480 | 481.1 | 481.1 | 486.5 |

* denotes degenerate eigenvalue.
The former five eigenvalues of the analytical solution, UT method, LM method and FEM obtained using ABAQUS for a square cavity with the Dirichlet and the Neumann boundary conditions

the two boundary conditions are termed the "Dirichlet" and "Neumann" types. The equation of state, *i.e.*, the constitutive behavior, is

$$K/\rho_0 = c^2, \tag{30}$$

where $\rho_0$ is the ambient density of the fluid, $K$ is the bulk modulus of the fluid, and $c$ is the speed of sound. For the case of air, we have

$$c = 340\, m/s. \tag{31}$$

In order to calculate the frequencies of an enclosed cavity, a standard linear eigenvalue problem can be obtained as follows:

$$[K]\mathbf{x} = -k^2\mathbf{x}, \tag{32}$$

where $[K]$ is a square symmetric matrix, and $\mathbf{x}$ is an eigenvector. As shown in Table 1, the eigenvalue problem of Eq. (32) is linear for FEM instead of nonlinear as in Eqs. (26)–(29) for BEM. Since the finite element method is employed in the ABAQUS code, $\mathbf{x}$ is the mode shape in the field instead of the boundary mode in BEM. Many eigenvalue solvers have been used in the literature. The subspace technique is employed in this paper.

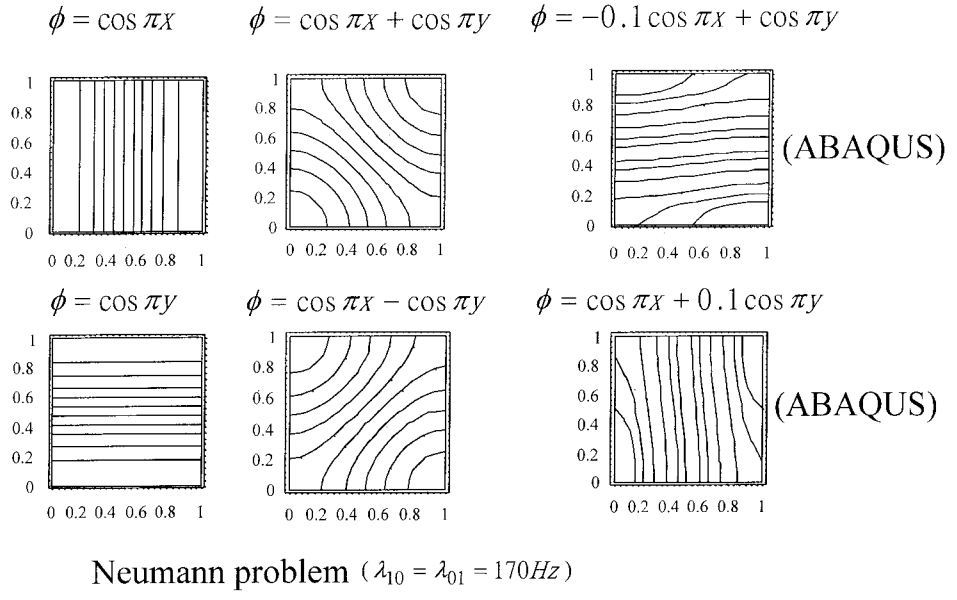


Fig. 1. Contour plot of the exact solution of the degenerate modes of the first eigenvalue 170 Hz for the Neumann problem.

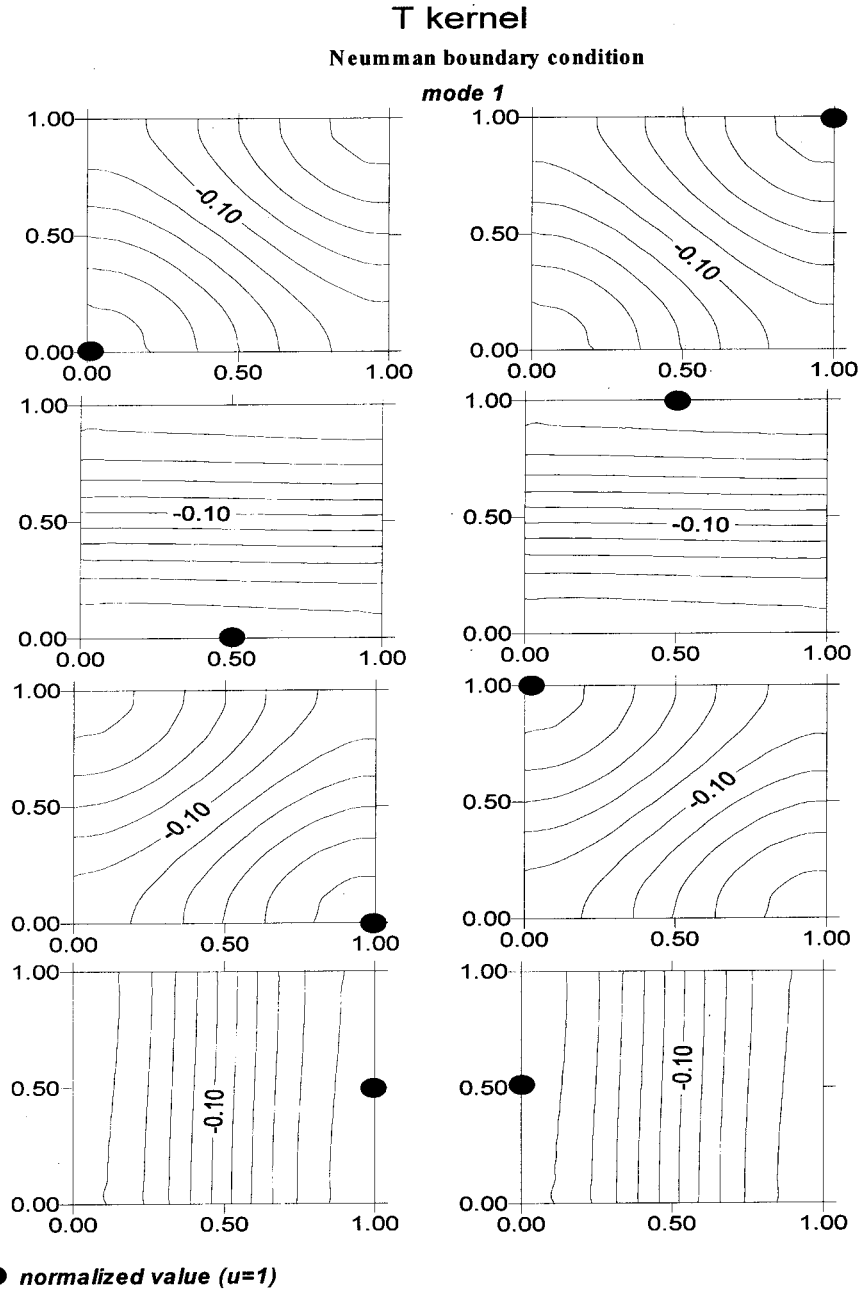


Fig. 2. (a) Contour plot of the degenerate modes of the first eigenvalue for the Neumann problem using the UT method.

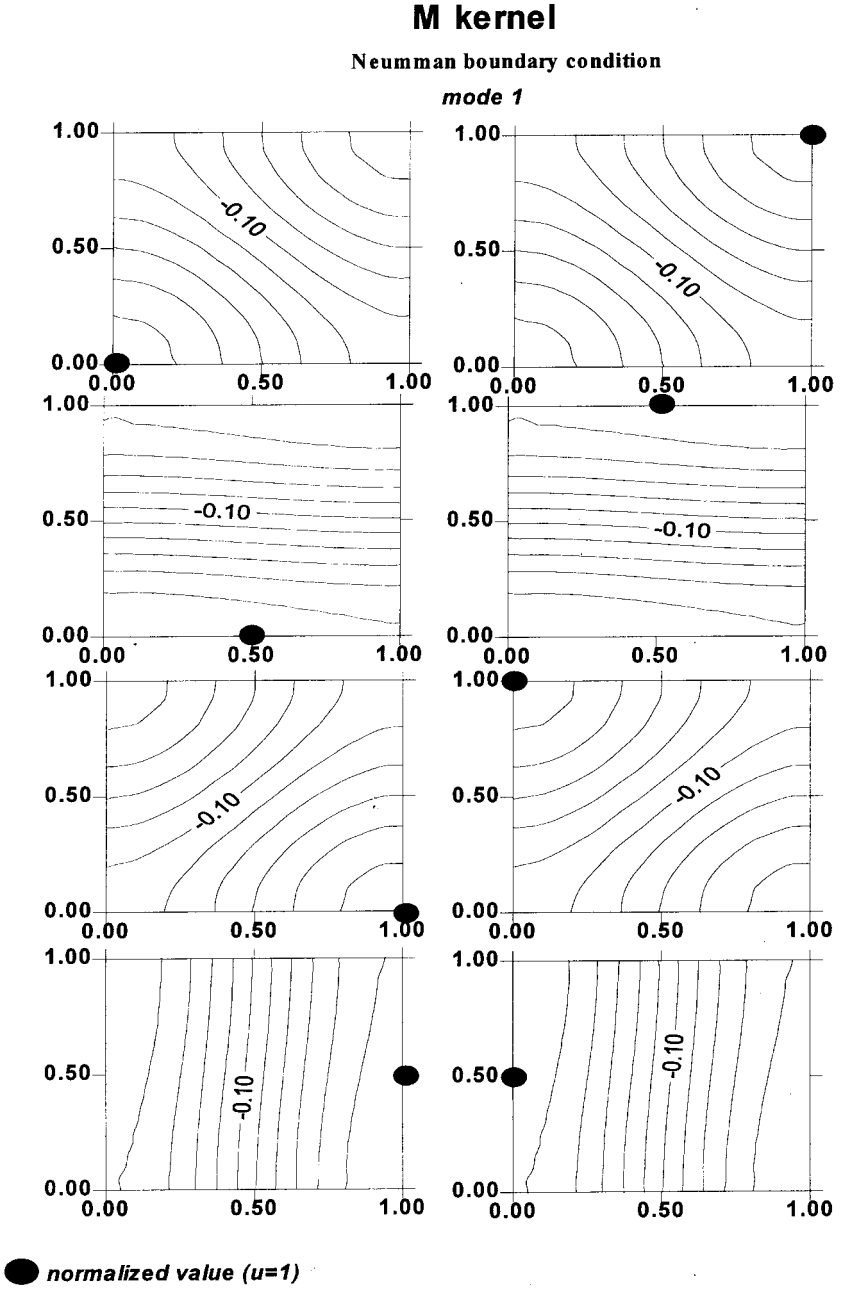


Fig. 2. (b) Contour plot of the degenerate modes of the first eigenvalue for the Neumann problem using the LM method.

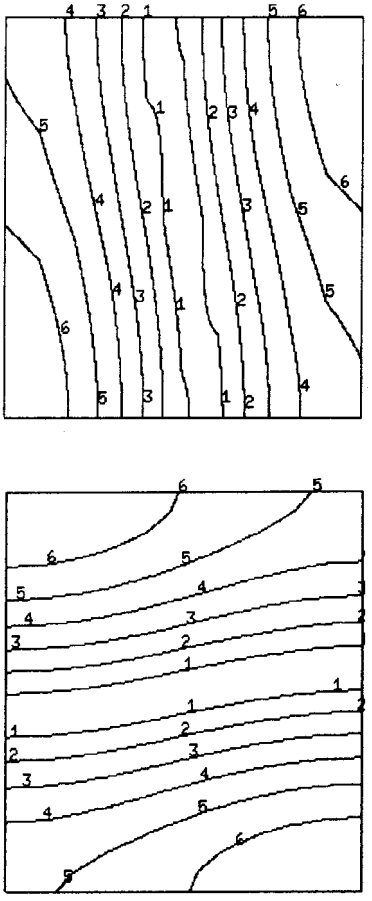

Fig. 2. (c) Contour plot of the degenerate modes of the first eigenvalue for the Neumann problem using ABAQUS.

## 6. Illustrative examples

**Example 1.** A square cavity with the Neumann boundary condition.

A square cavity of area $\ell^2 m^2$ with the Neumann boundary condition will be considered as a demonstrative example. The former five eigenvalues are shown in Table 2 for $l=1$. Analytical solutions and numerical results obtained using the UT and LM methods are both shown. Also, the FEM results obtained using ABAQUS have been worked out for comparison. The analytical solution of the eigenvalue is

$$k_{mn}=\pi\sqrt{\left(\frac{m}{l}\right)^2+\left(\frac{n}{l}\right)^2}, \quad (m=0,1,2,3,\ldots,n=0,1,2,3,\ldots), \tag{33}$$

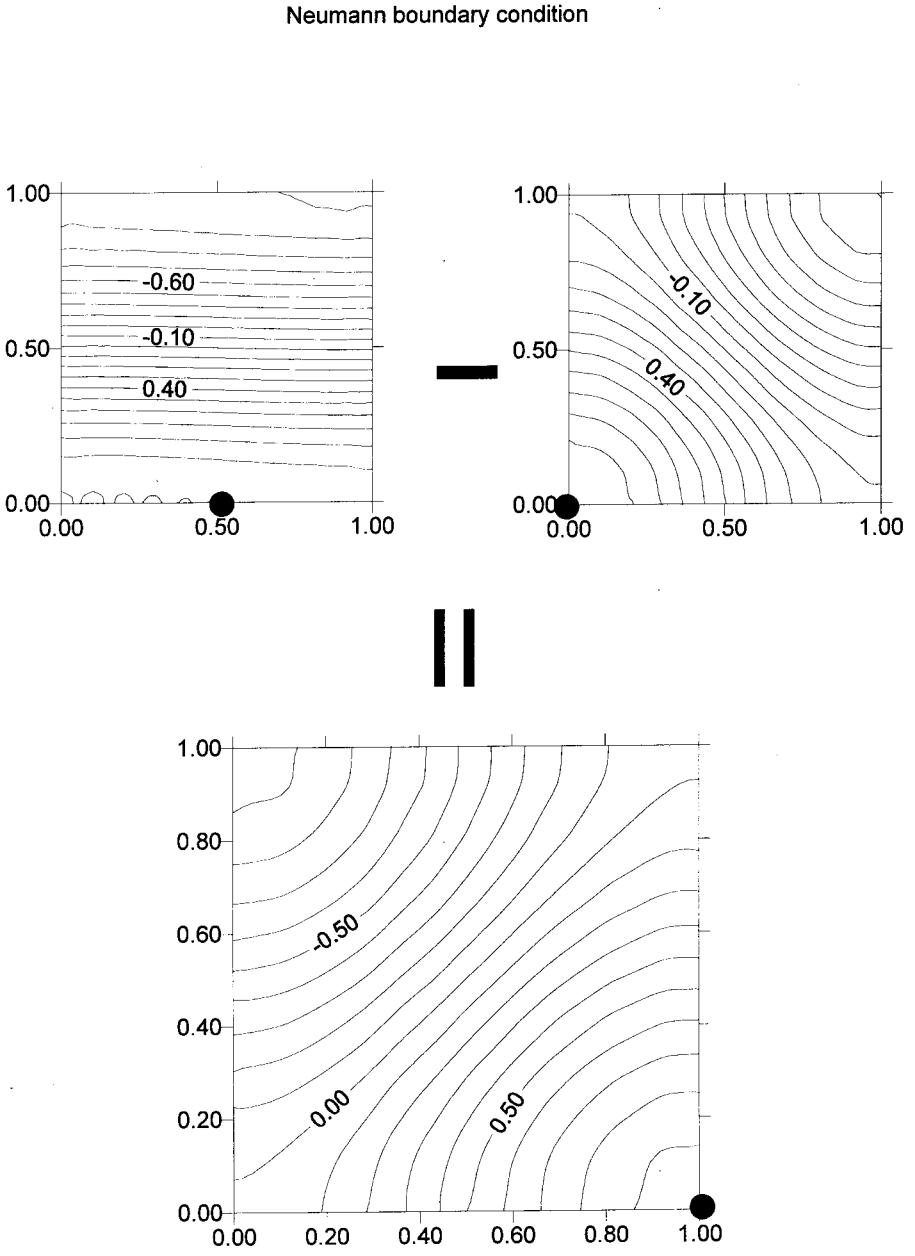


Fig. 3. A linear combination of two independent degenerate modes.

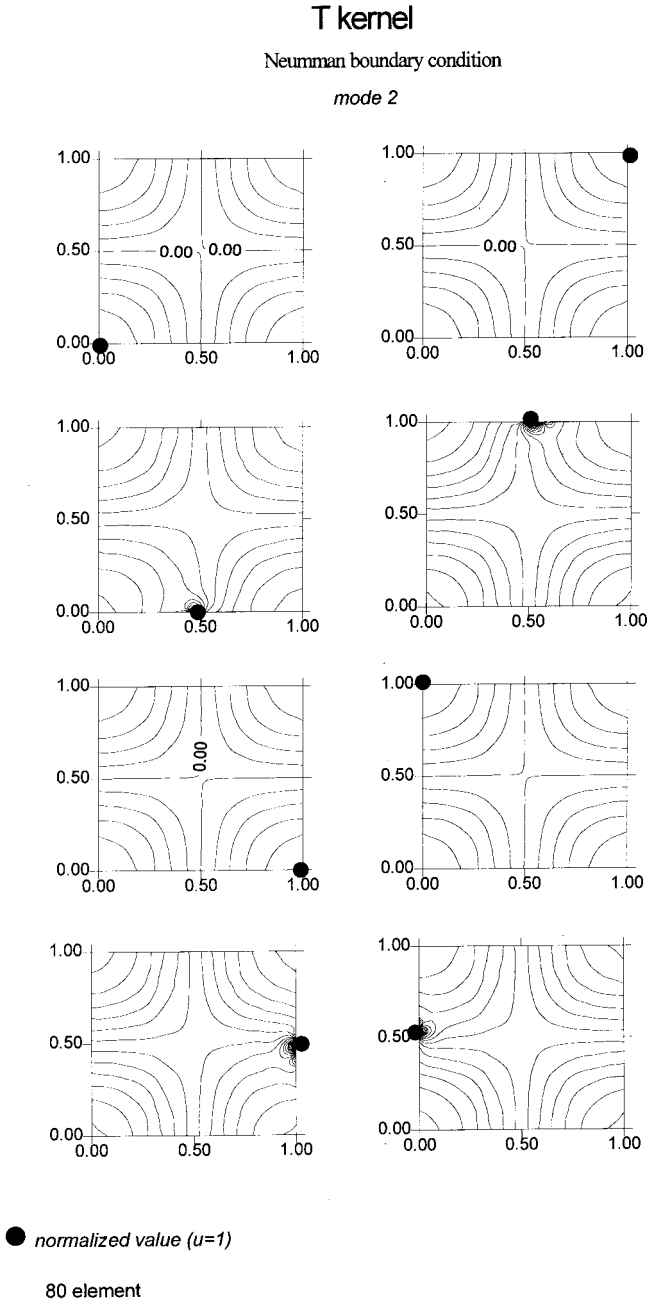


Fig. 4. (a) Sensitivity in determining the mode of the second eigenvalue 240.4 Hz for the Neumann problem by specifying the normalized value near the node using the UT method (80 elements).

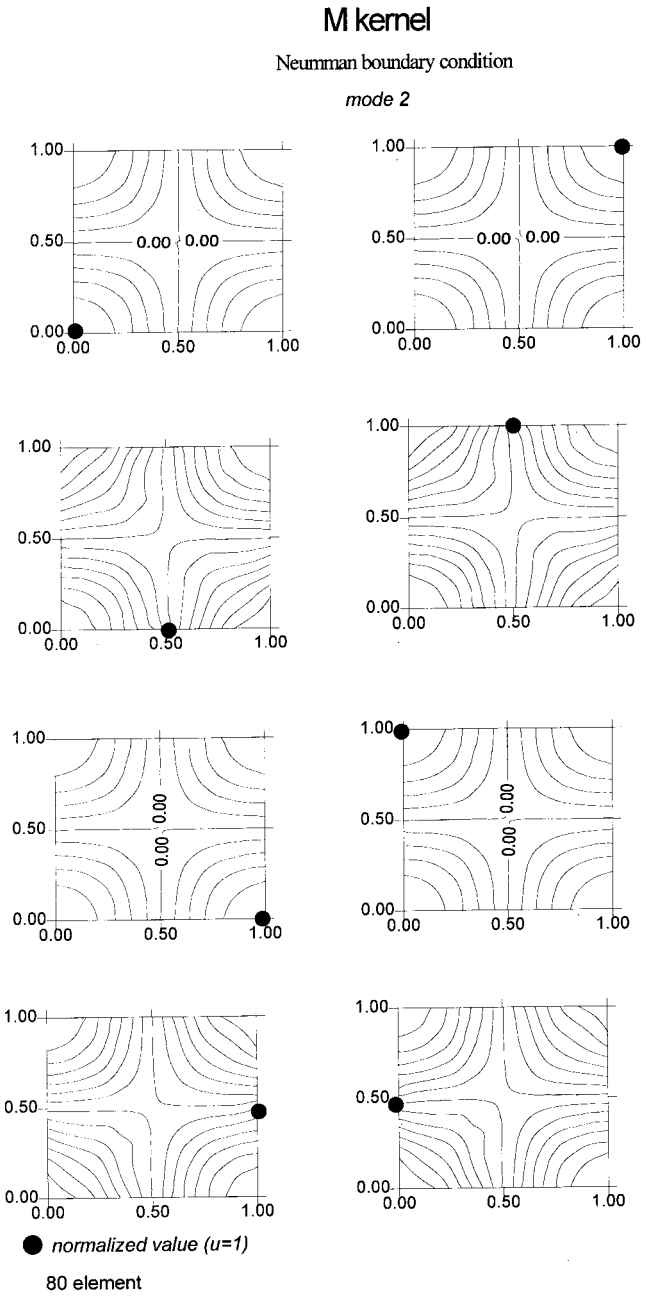


Fig. 4. (b) Sensitivity in determining the mode of the second eigenvalue 240.4 Hz for the Neumann problem by specifying the normalized value near the node using the LM method (80 elements).

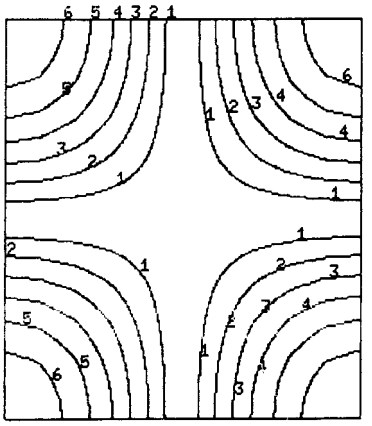

Fig. 4. (c) Contour plot of the node of the second eigenvalue 240.4 Hz for the Neumann problem using ABAQUS.

and its corresponding degenerate eigenfunctions can be expressed as $a\beta_m(x_1, x_2) + b\beta_m(x_1, x_2)$, where $a$ and $b$ are real numbers, and $\beta_m(x_1, x_2)$ is the analytical solution of the eigenfunction as shown below.

$$\beta_m(x_1, x_2) = \cos\left(\frac{m\pi x_1}{l}\right)\cos\left(\frac{n\pi x_2}{l}\right), \quad (m=0, 1, 2, 3, \ldots, n=0, 1, 2, 3, \ldots). \tag{34}$$

The rigid mode ($m=0$, $n=0$) resulting from a zero eigenvalue is not considered here. Both the (0,1) and (1,0) modes are degenerate eigenfunctions for the first eigenvalue of 170 Hz with multiplicity two as shown in Table 2. The analytical solutions for the modes corresponding to the first eigenvalue in the contour are shown in Fig. 1. Using the UT method, we obtained the degenerate modes by specifying a normalized value of one for boundary data at different locations. Also, the same modes could be obtained using the LM method. The results are shown in Fig. 2(a) and (b) for the UT and LM methods, respectively, where the dark circle "•" denotes the specified position of the normalized boundary data. Both Fig. 2(a) and (b) indicate that the degenerate mode depends on the specified location of the normalized data. It is found that the maximum value of the obtained mode occurs at the specified position. For comparison, Fig. 2(c) shows the degenerate modes obtained using ABAQUS. Fig. 2(a)–(c) all indicate that distortion appears in comparison with the exact solution in Fig. 1. The ABAQUS results listed in Fig. 2(c) show that the obtained modes are the linear combinations, (–0.1, 1) and (1, 0.1), of the two independent modes of the exact solution in Fig. 1, respectively. Also, a linear combination for the two independent degenerate modes obtained using dual BEM is used to construct another mode in Fig. 3. For the case of nondegenerate (1,1) eigenfunctions of the second eigenvalue 240.4 Hz, the same eigenmode was obtained even when the

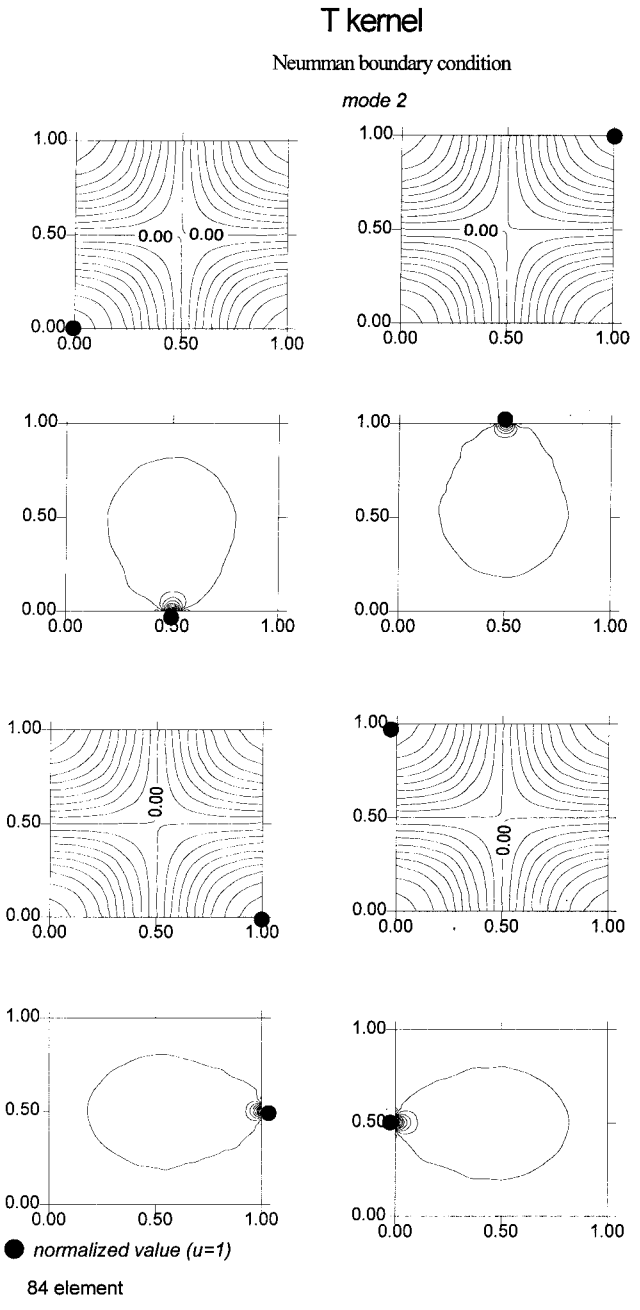


Fig. 5. (a) Failure in determining the mode of the second eigenvalue 240.4 Hz for the Neumann problem by specifying the normalized value on the node using the UT method (84 elements).

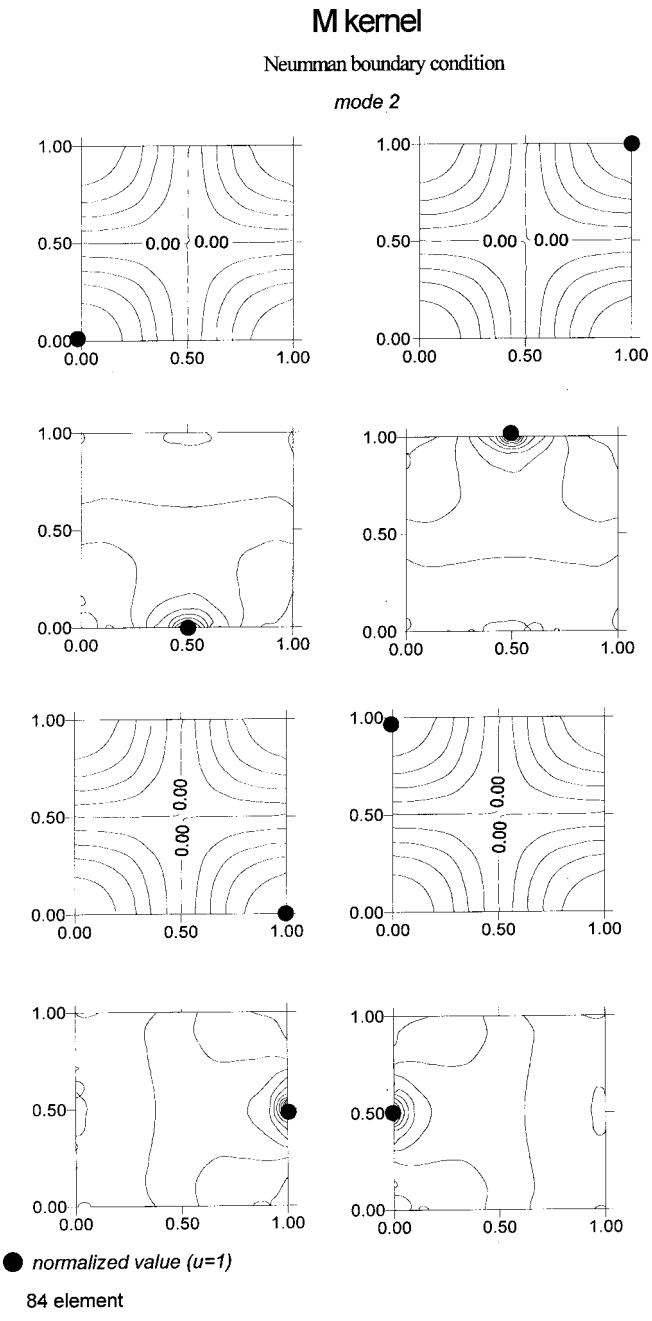


Fig. 5. (b) Failure in determining the mode of the second eigenvalue 240.4 Hz for the Neumann problem by specifying the normalized value on the node using the LM method (84 elements).

position of the boundary data having a value of one was changed except to the locations of at the node and near the node. To demonstrate this point, Fig. 4(a) shows the sensitivity in determining the mode corresponding to the second eigenvalue by specifying the normalized value near the node using the UT method (80 elements). Fig. 4(b) shows the sensitivity in determining the same mode by specifying the normalized value near the node using the LM method (80 elements). For comparison, Fig. 4(c) shows the same mode obtained using ABAQUS. Also, Fig. 5(a) shows the failure in determining the same mode by specifying the normalized value on the node using the UT method (84 elements). Fig. 5(b) shows the failure in determining the same mode by specifying the normalized value on the node using the LM method (84 elements). Since the constant element scheme was used, two meshes, 80 elements in Fig. 4(a) and (b) and 84 elements in 5(a) and 5(b) were provided to specify the normalized data on the boundary locations, near the node and on the node, respectively. Both cases illustrate the sensitivity and failure in determining the mode. As shown in Fig. 4(a), (b), Fig. 5(a) and (b), the same mode was obtained if the position of the normalized data was not on the node or near the node. For the degenerate (0,2) and (2,0) modes of the third eigenvalue 340 Hz, Fig. 6 shows the contour plot of the exact solution of some possible degenerate modes. Fig. 7(a) shows the contour plot of the degenerate modes obtained using the UT method. Fig. 7(b) shows the contour plot of the degenerate modes obtained using the LM method. For comparison, Fig. 7(c) shows the degenerate modes obtained using ABAQUS. The two modes are combinations of two analytical solutions with

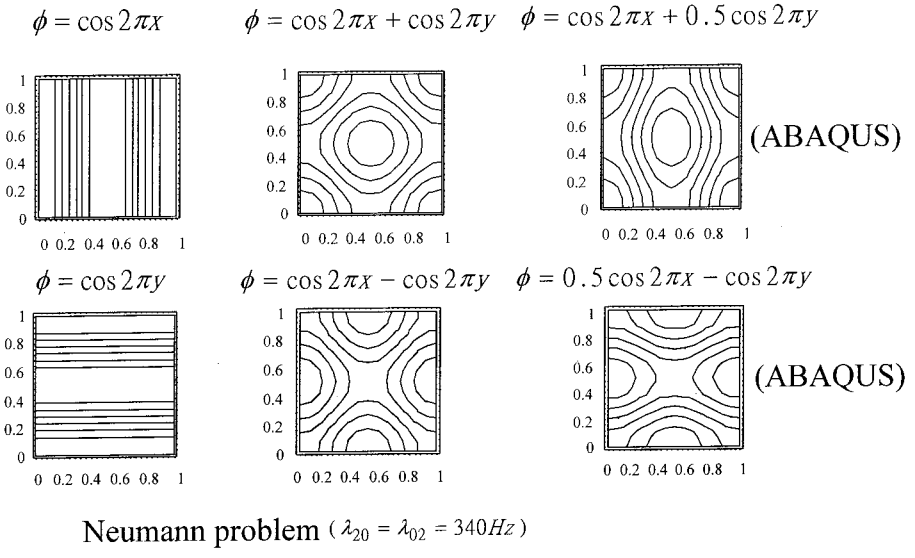


Fig. 6. Contour plot of the exact solution of the degenerate modes of the third eigenvalue 340 Hz for the Neumann problem.

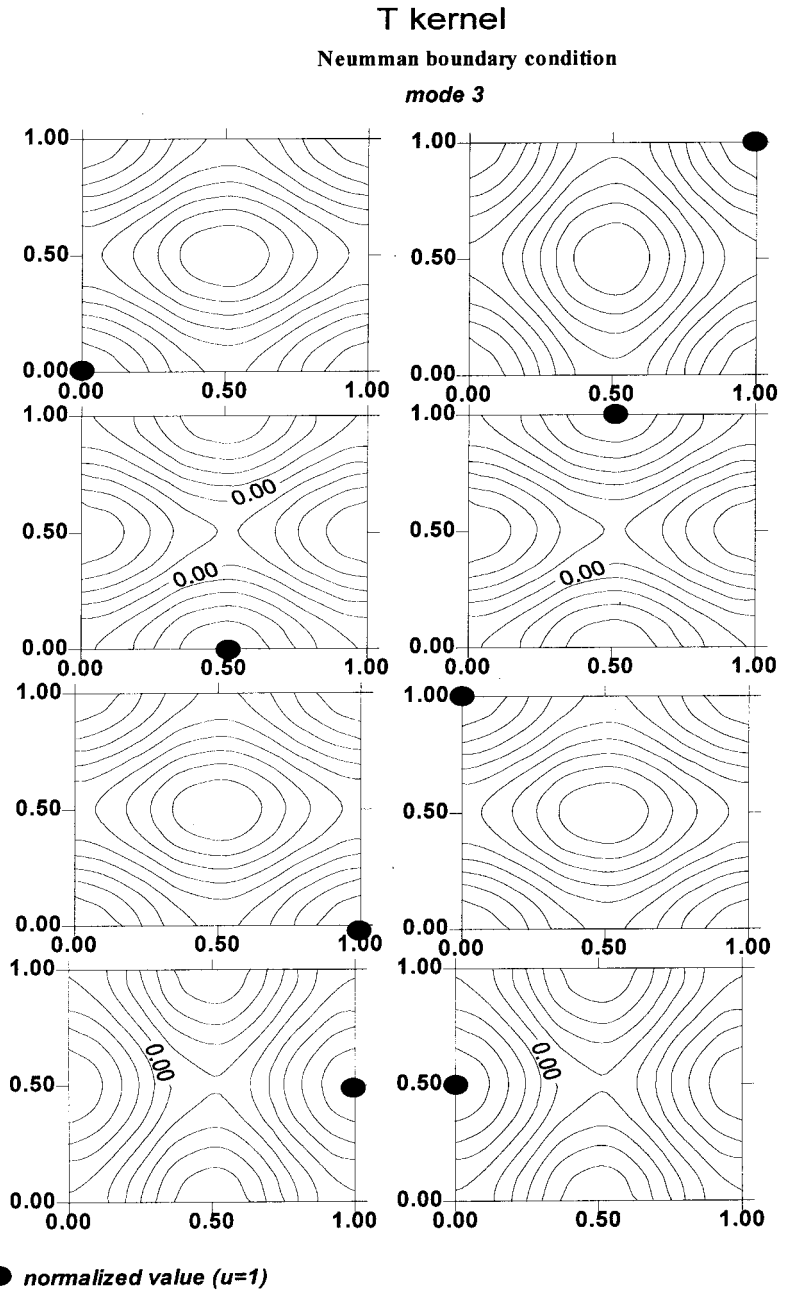


Fig. 7. (a) Contour plot of the degenerate modes of the third eigenvalue for the Neumann problem using the UT method.

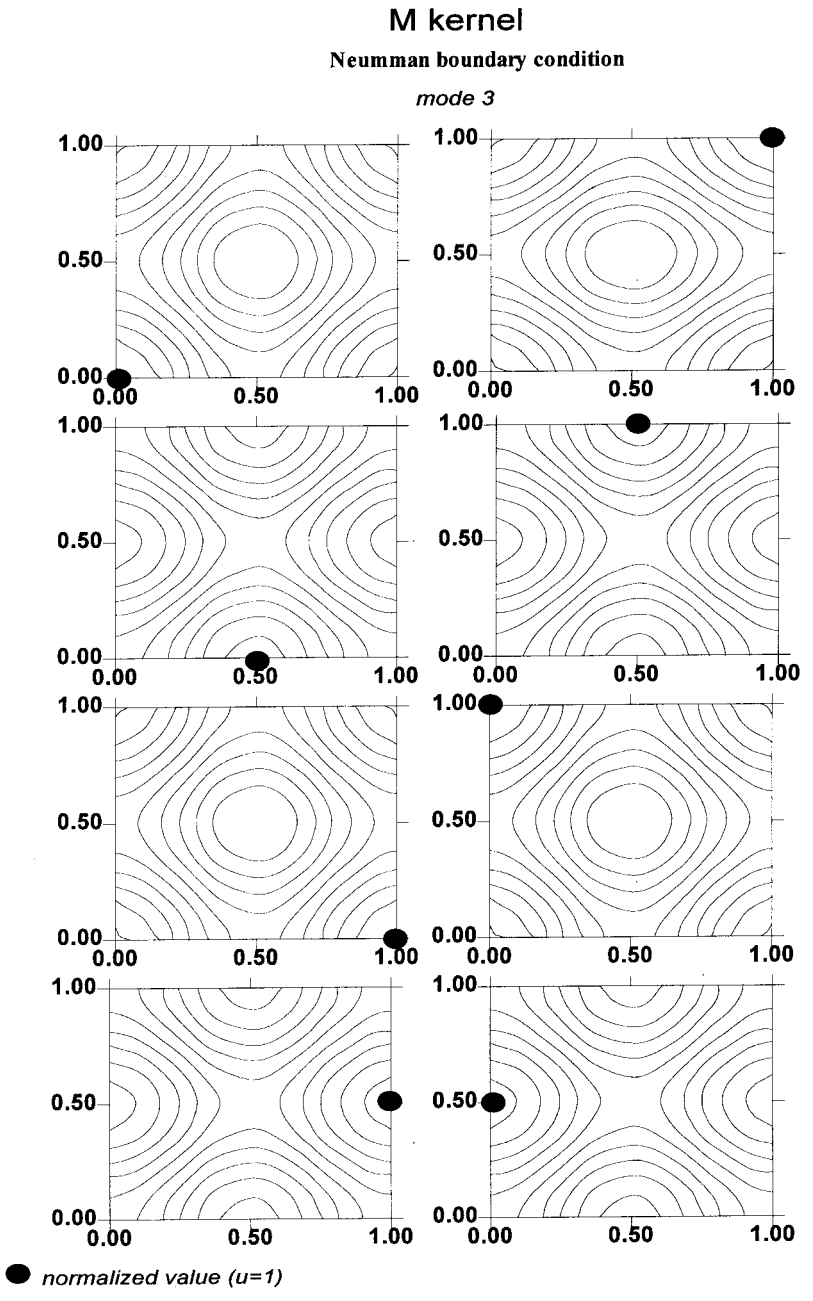


Fig. 7. (b) Contour plot of the degenerate modes of the third eigenvalue for the Neumann problem using the LM method.

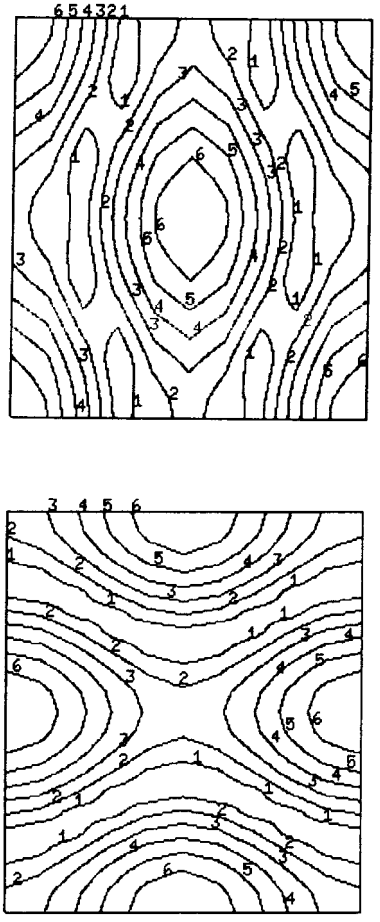

Fig. 7. (c) Contour plot of the degenerate modes of the third eigenvalue for the Neumann problem using ABAQUS.

coefficients of (1, 0.5) and (0.5, –1) as in Fig. 6. It is found that dual BEM (UT and LM) and FEM, using ABAQUS, can obtain at least these two possible degenerate modes.

**Example 2.** A square cavity with the Dirichlet boundary condition.

A square cavity of area $\ell^2$-$n^2$ with the Dirichlet boundary condition will be considered next. The former five eigenvalues are also shown in Table 2 for $l = 1$. Analytical solutions and numerical results obtained using the UT and LM methods are both shown. Also, results obtained using ABAQUS were worked out for comparison. The analytical solution of the eigenvalue is

$$k_{mn}=\pi\sqrt{\left(\frac{m}{l}\right)^2+\left(\frac{n}{l}\right)^2},\ (m=1,2,3,\ldots,n=1,2,3,\ldots), \tag{35}$$

and its corresponding degenerate eigenfunctions can be represented by $a\rho_{mn}(x_1,x_2)+b\rho_{nm}(x_1,x_2)$, where $a$ and $b$ are real numbers, and $\rho_{mn}(x_1,x_2)$ is the analytical solution of the eigenfunction as shown below.

$$\rho_{mn}(x_1,x_2)=\sin\left(\frac{m\pi x_1}{l}\right)\sin\left(\frac{n\pi x_2}{l}\right),\ (m=1,2,3,\ldots,n=1,2,3,\ldots). \tag{36}$$

Both the (1,2) and (2,1) modes are degenerate eigenfunctions for the second eigenvalue 380.1 Hz in Table 2. The analytical solutions for the possible degenerate modes in the contour are shown in Fig. 8. Using the UT method, we obtained the degenerate modes by specifying a value of one for the corresponding boundary data at different locations shown in Fig. 9(a). Also, the same modes could be obtained using LM method in Fig. 9(b). Both Fig. 9(a) and (b) show that the eigenfunctions could be distinguished by specifying the normalized data at different boundary positions. Both Fig. 9(a) and (b) indicate that the degenerate mode depends on the specified location of the normalized data. It is also found that the maximum value of the obtained mode occurs at the position where the normalized data is specified. For comparison, Fig. 9(c) shows the degenerate modes obtained using ABAQUS. The

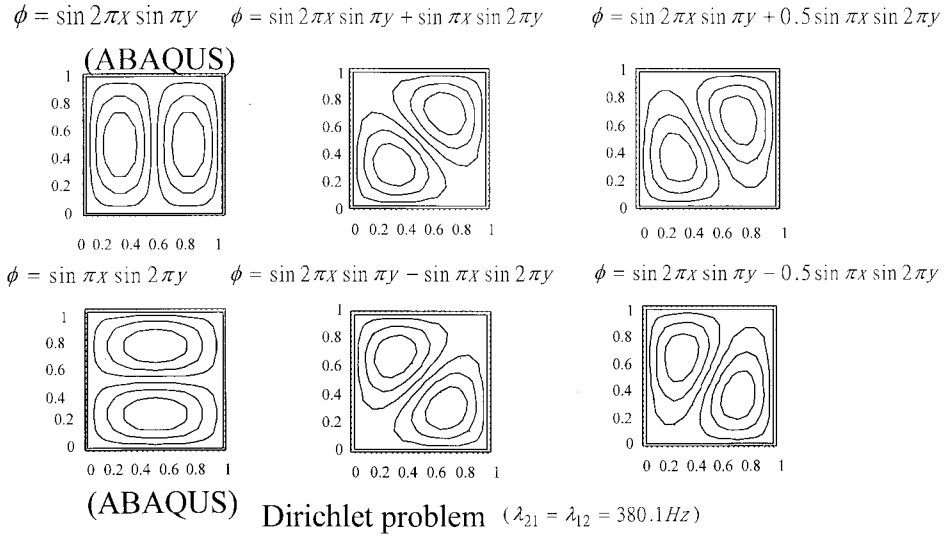


Fig. 8. Contour plot of the exact solution of the degenerate modes of the second eigenvalue 380.1 Hz for the Dirichlet problem.

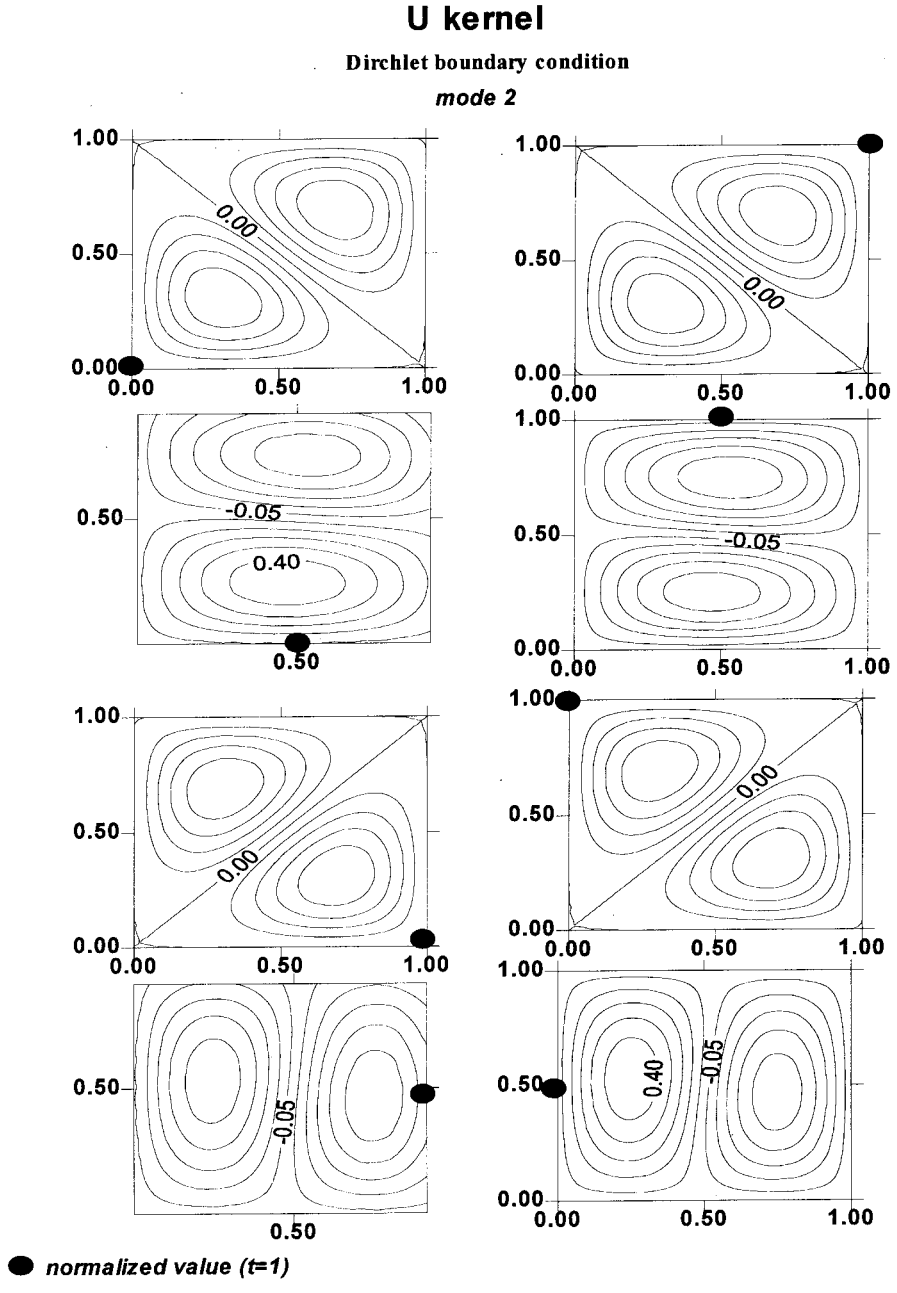


Fig. 9. (a) Contour plot of the degenerate modes of the second eigenvalue for the Dirichlete problem using the UT method.

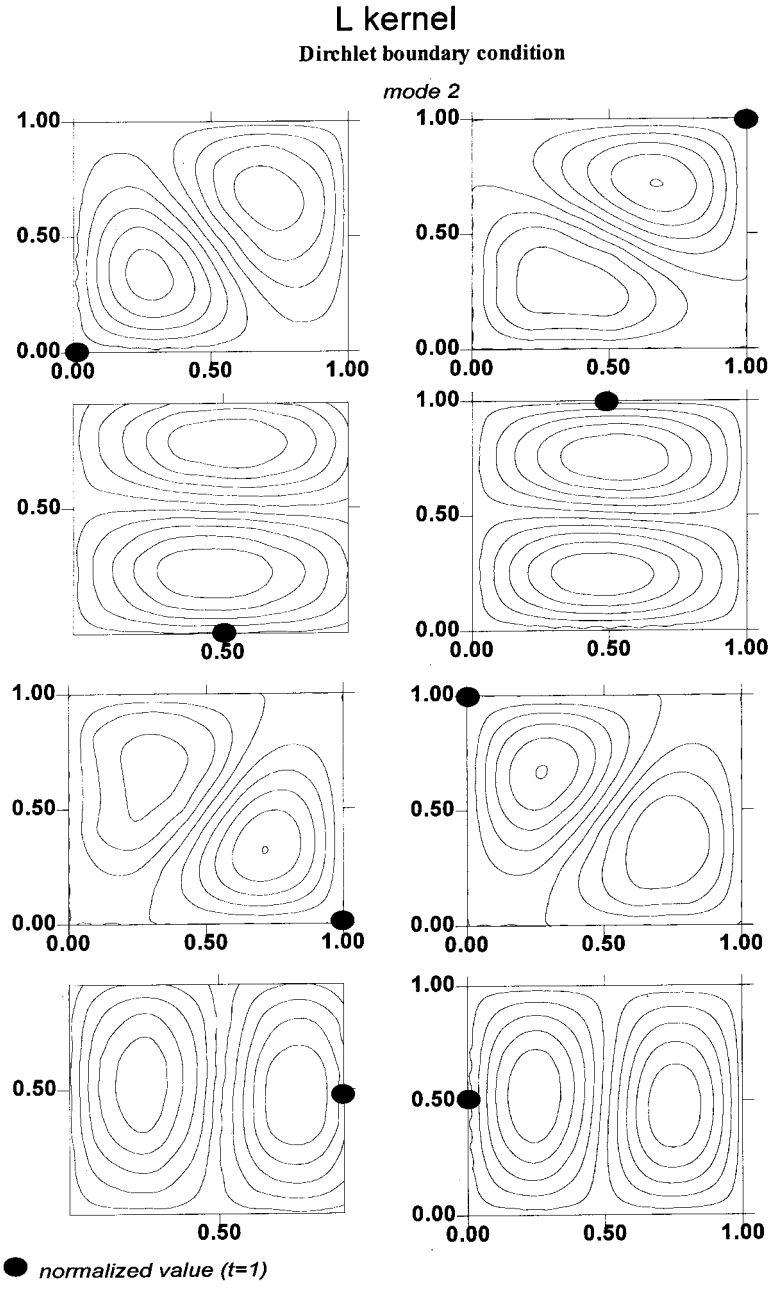


Fig. 9. (b) Contour plot of the degenerate modes of the second eigenvalue for the Dirichlet problem using the LM method.

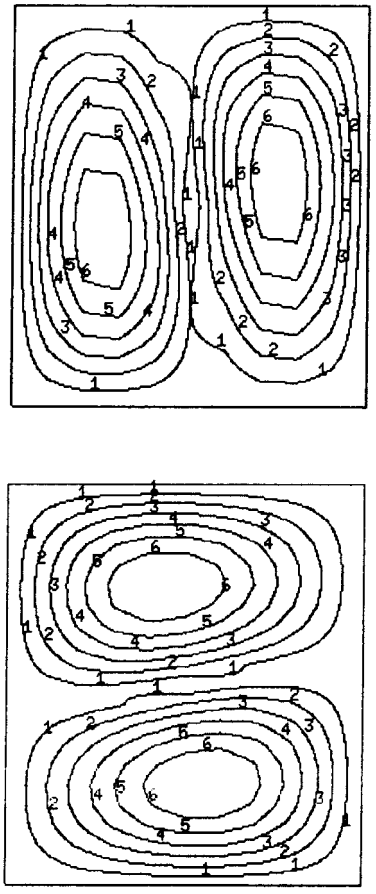

Fig. 9. (c) Contour plot of the degenerate modes of the second eigenvalue for the Dirichlet problem using ABAQUS.

two modes are similar to the analytical solutions shown in Fig. 8. It is found that dual BEM (UT and LM) and FEM using ABAQUS can obtain the two independent degenerate modes. For the degenerate modes corresponding to the fourth eigenvalue, 537.6 Hz, as shown in Table 2, the exact solution is shown in Fig. 10. In the same way, Fig. 11(a) and (b) show the modes obtained using the UT and LM methods, respectively. Both Fig. 11(a) and (b) also indicate that the eigenfunctions can be distinguished by specifying the normalized data at different boundary positions. It is interesting to find that the modes obtained using both the UT and LM methods are different even though the specified locations of the normalized data of value one are the same. This finding shows that the LM method can also be used to distinguish whether the eigenvalue is degenerate or not in spite of the change of the

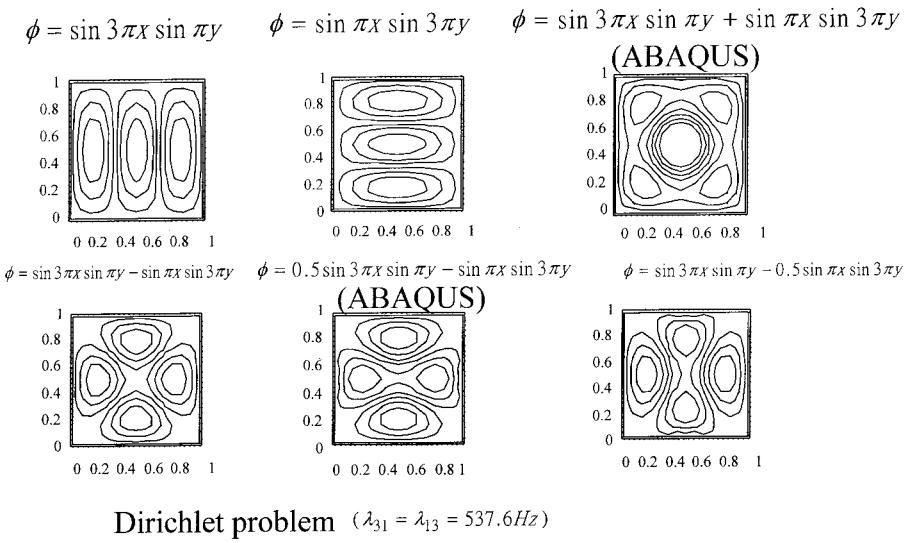


Fig. 10. Contour plot of the exact solution of the degenerate modes of the fourth eigenvalue 537.6 Hz for the Dirichlet problem.

position of the normalized data. In addition, the FEM results obtained using ABAQUS are shown in Fig. 11(c). The two modes are combinations of the two basic modes in the analytical solutions of Fig. 10 with the coefficients (1, 1) and (0.5, –1). Fig. 11(a)–(c) show that dual BEM (UT and LM) and FEM using ABAQUS can obtain at least two possible degenerate modes.

## 7. Conclusion

The dual formulation for the eigenvalue problem of acoustics has been derived. Numerical experiments on degenerate eigenfunctions have been performed using dual BEM. By specifying the appropriate locations for the normalized data, we can obtain the degenerate eigenfunctions. Also, this method can be used to distinguish whether the eigenvalue is degenerate or not. Two examples, a square cavity with Dirichlet and Neumann boundary conditions, have been given to show the validity of the present method. The present results have been compared with those of the analytical solution and of FEM using ABAQUS. Good agreement has been obtained.

## Acknowledgements

Financial support from the National Science Council, under Grant No.NSC-86-2211-E-019-006, for National Taiwan Ocean University is gratefully acknowledged.

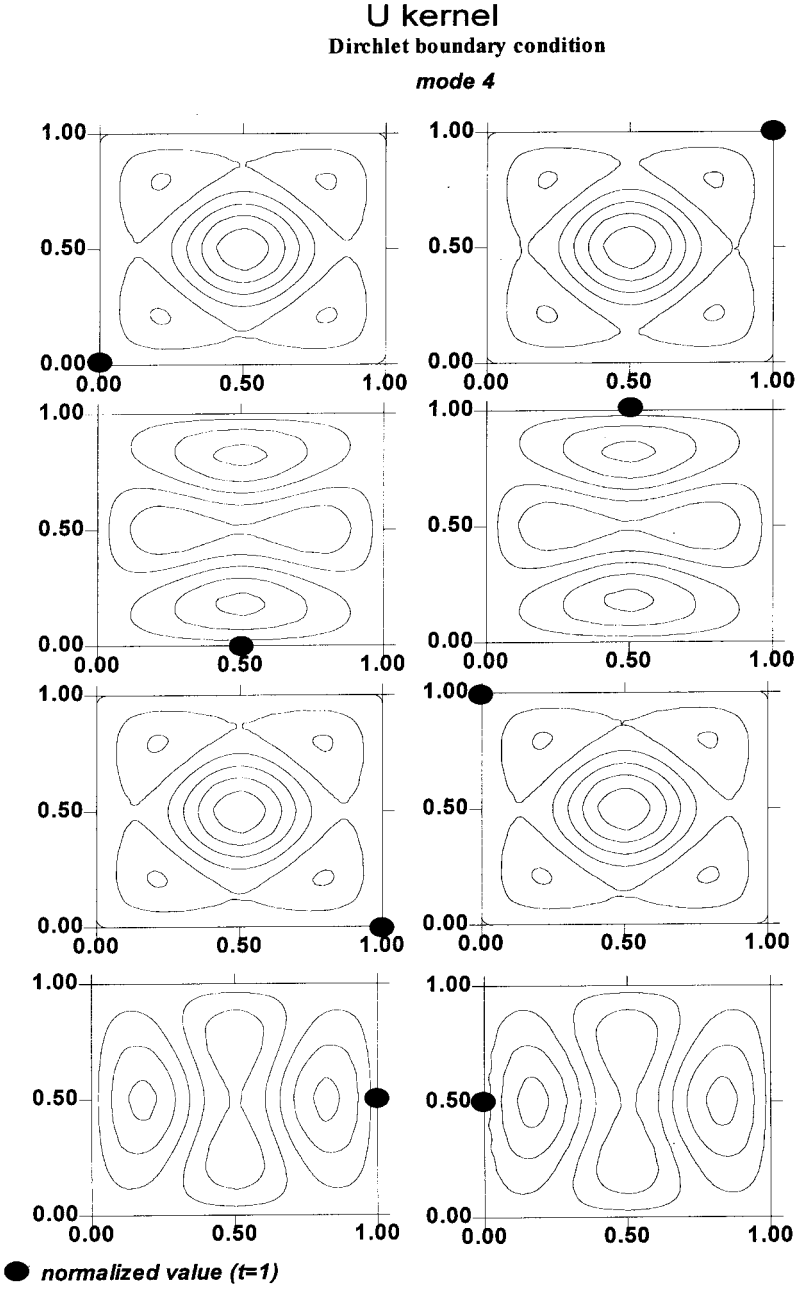


Fig. 11. (a) Contour plot of the degenerate modes of the fourth eigenvalue for the Dirichlete problem using the UT method.

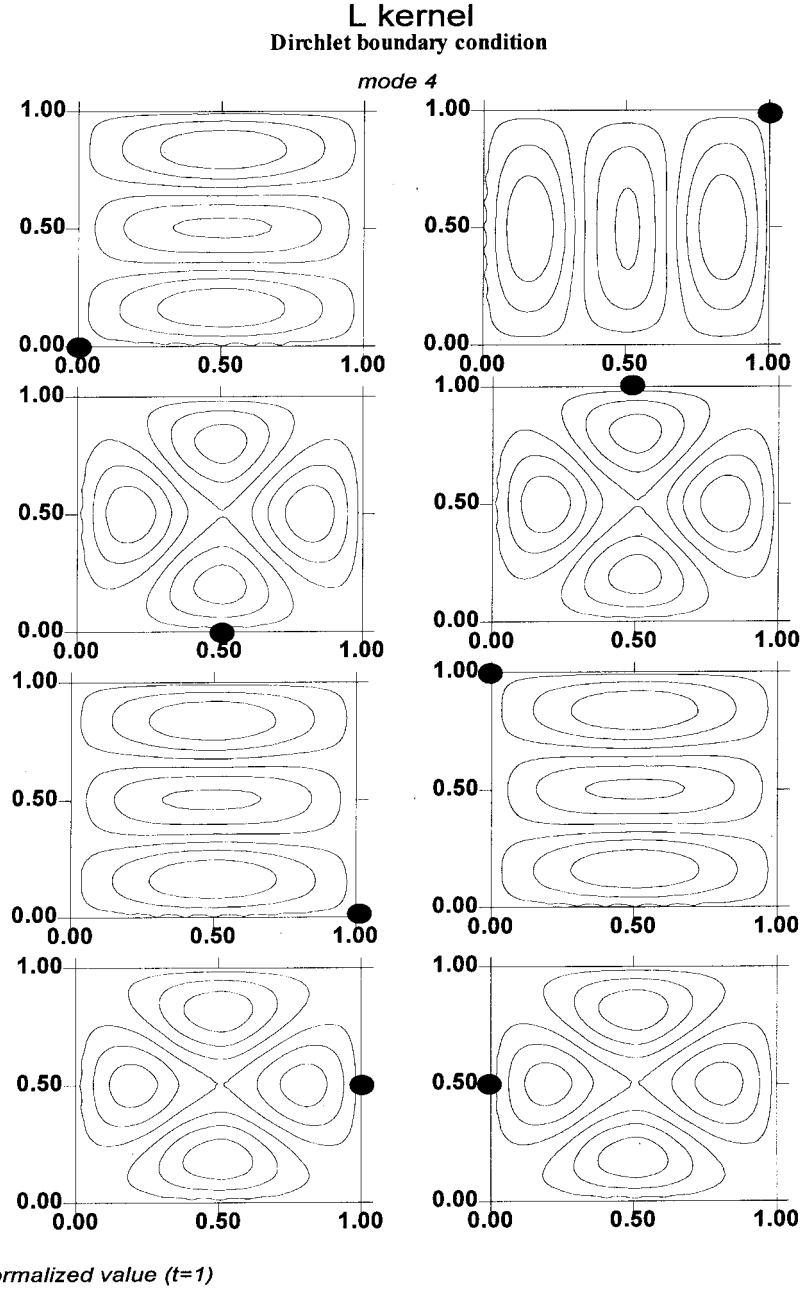


Fig. 11. (b) Contour plot of the degenerate modes of the fourth eigenvalue for the Dirichlet problem using the LM method.

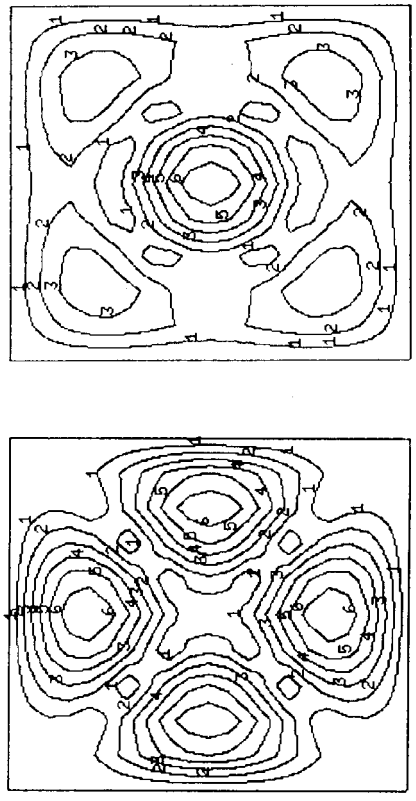

Fig. 11. (c) Contour plot of the degenerate modes of the fourth eigenvalue for the Dirichlet problem using ABAQUS.

## References

[1] Kopuz S, Lalor N. Analysis of interior acoustic fields using the finite element method and boundary element method. Applied Acoustics 1995;45:193–210.
[2] Hadamard J. Lectures on Cauchy's problem in linear partial differential equations. New York: Dover, 1952.
[3] Mangler KW. Improper integrals in theoretical aerodynamics. RAE Report No. 2424, 1951.
[4] Tuck EO. Application and solution of Cauchy singular integral equations. In: Anderson RS et al., editors. The application and numerical solution of integral equations. Sijthoff: Noordhoff, 1980.
[5] Cheng-Sheng Wang, Sing Chu, Jeng-Tzong Chen. Boundary element method for predicting store airloads during its carriage and separation procedures. In: Grilli et al. editor. Computational engineering with boundary elements, vol.1, Fluid and Potential Problems, CMP, 1990.
[6] Hong H-K, Chen JT. Derivations of integral equations in elasticity. Journal of ASCE 1988 Em5;114(6):1028–44.
[7] Chen, JT. On Hadamard principal value and boundary integral formulation of fracture mechanics. Master Thesis of Institute of Applied Mechanics, National Taiwan University, Taiwan, 1986.

[8] Hong H-K, Chen JT. Generality and special cases of dual integral equations of dual integral equations of elasticity. J CSME 1989;9(1):1–19.
[9] Chen JT, Hong H-K. On Hadamard principal value and its application to crack problems through BEM. In: Proceedings of The 11th National Conference on Theo. and Appl. Mech., Taiwan, 1987.
[10] Portela A, Aliabadi MH, Rooke DP. The dual boundary element method: effective implementation for crack problems. Int J Num Meth Eng 1992;33:1269–87.
[11] Mi Y, Aliabadi MH. Dual boundary element method for three-dimensional fracture mechanics analysis. Eng Anal with Bound Elem 1992;10:161–71.
[12] Chen JT, Hong H-K. Application of integral equations with superstrong singularity to steady state heat conduction. Thermochimica Acta 1988;135:133–8.
[13] Chen JT, Hong H-K. Singularity in Darcy flow around a cutoff wall. In: Brebbia CA, Conner JJ, editors. Advances in boundary elements, vol 2. Field and Flow Solution, 1989:15–27.
[14] Gray LJ. Boundary element method for regions with thin internal cavities. Engineering Analysis with Boundary Elements 1989;6(4):180–4.
[15] Terai T. On calculation of sound field around three dimensional objects by integral equation method. J Sound and Vibration 1980;69:71–100.
[16] Wu TW, Wan GC. Numerical modelling of acoustic radiation and scattering from thin bodies using a Cauchy principal integral equation. J Acoust Soc Amer 1992;92:2900–6.
[17] Chen JT, Chen KH. Dual integral formulation for determining the acoustic modes of a two-dimensional cavity with a degenerate boundary. Engineering Analysis with Boundary Elements. 1998;21:105–16.
[18] Chen KH, Chen JT, Liou DY. Dual boundary element analysis for a acoustic cavity with an incomplete partition. The Chinese Journal of Mechanics 1998;14:1:11.
[19] Chen JT, Hong H-K. Dual boundary integral equations at a corner using contour approach around singularity. Advances in Engineering Softwares 1994;21(3):169–78.
[20] Liang MT, Chen JT, Yang SS. Error estimation for boundary element method, Engineering Analysis with Boundary Elements, Accepted 1998.
[21] Chen JT, Liang MT, Yang SS. Dual boundary integral equations for exterior problems. Engineering Analysis with Boundary Elements 1995;16:33–340.
[22] Martin PA, Rizzo FJ, Gonsalves IR. On hypersingular integral equations for certain problems in mechanics. Mech Res Commun 1989;16(2):65–71.
[23] Chen JT, Hong H-K. Review of dual integral representations with emphasis on hypersingularity and divergent series, Invited one-hour Lecture. In: Proceedings of the Fifth International Colloquium on Numerical Analysis, Plovdiv, Bulgaria, 1996. (This note will appear in Appl Mech Rev, Vol. 52, 1999).
[24] Chen JT, Hong H-K. Boundary Element Method, 2nd ed., Taipei Taiwan: New World Press, 1992 (in Chinese).
[25] Chen JT, Hong H-K. On the dual integral representation of boundary value problem in Laplace equation. Boundary Element Abstracts 1993;3:114–16.
[26] Günter NM. Potential theory and its applications to basic problems of mathematical physics. New York: Frederick Ungar, 1967.
[27] Buecker HF, Field singularities and related integral representations. In: Sih GC, editor. Mechanics of Fracture, vol. 1, 1973.
[28] Tanaka M, Sladek V, Sladek J. Regularization techniques applied to boundary element methods. Appl Mech Rev 1994;47(10): 457–99.
[29] Burton AJ, Miller GF. The application of integral equation methods to numerical solution of some exterior boundary value problems. Proc of Roy Soc London Ser A 1971;323:201–10.
[30] Chen KH. Applications of dual integral equations to acoustic problems. Master thesis, Department of Harbor and River Engineering, National Taiwan Ocean University, Taiwan, 1997.
[31] Fetter AL, Walecka JD. Theoretical mechanics of particles and continua. New York: McGraw-Hill, 1980.
[32] Kamiya N, Wu ST. Generalized eigenvalue formulation of the Helmholtz equation by the Trefftz method. Engineering Computations 1994;11:177–86.

[33] Chen JT, Wong, FC. Dual formulation for multiple reciprocity method for the acoustic mode of a cavity with a thin partition, J Sound and Vibration, Accepted, 1998.
[34] Gladwell GML, Willms NB. On the mode shapes of the Helmholtz equation. J Sound and Vibration 1995;188(3):419–33.
[35] Laura PAA, Bambill DV, Jederlinic V. Comments on the mode shapes of the Helmholtz equation. J Sound and Vibration 1997; 199(5):813–5.
[36] Lin TW, Shiau HT, Huang JT. Singular decomposition by adding dummy links and dummy degrees. J Chinese Institute of Engineers 1992;15(6):723–7.
[37] MSC/ABAQUS User Manual, MSC Version 5.5, 1996.